

**Repository of the Max Delbrück Center for Molecular Medicine (MDC)  
in the Helmholtz Association**

<https://edoc.mdc-berlin.de/17087/>

**A gain-of-function mutation in the CLCN2 chloride channel gene causes  
primary aldosteronism**

---

Fernandes-Rosa F.L., Daniil G., Orozco I.J., Göppner C., El Zein R., Jain V., Boulkroun S.,  
Jeunemaitre X., Amar L., Lefebvre H., Schwarzmayr T., Strom T.M., Jentsch T.J., Zennaro M.C.

This is the final version of the accepted manuscript. The original article has been published in final edited form in:

Nature Genetics  
2018 MAR; 50(3), 355–361  
2018 FEB 05 (first published online: final publication)  
Doi: [10.1038/s41588-018-0053-8](https://doi.org/10.1038/s41588-018-0053-8)

URL: <https://www.nature.com/articles/s41588-018-0053-8>

Publisher: [Nature America](#) (Springer Nature)  
Copyright © 2018 Nature America Inc., part of Springer Nature. All rights reserved.

Publisher's notice

This is a post-peer-review, pre-copyedit version of an article published in *Nature Genetics*. The final authenticated version is available online at: <https://dx.doi.org/10.1038/s41588-018-0053-8>.

## **A gain-of-function mutation in the *CLCN2* chloride channel gene causes primary aldosteronism**

Fabio L Fernandes-Rosa<sup>1,2,3\*#</sup>, Georgios Daniil<sup>1,2\*</sup>, Ian J Orozco<sup>4,5\*</sup>, Corinna Göppner<sup>4,5§</sup>, Rami El Zein<sup>1,2§</sup>, Vandana Jain<sup>6^</sup>, Sheerazed Boulkroun<sup>1,2^</sup>, Xavier Jeunemaitre<sup>1,2,3</sup>, Laurence Amar<sup>1,2,7</sup>, Hervé Lefebvre<sup>8,9,10</sup>, Thomas Schwarzmayr<sup>11</sup>, Tim M Strom<sup>11,12</sup>, Thomas J Jentsch<sup>4,5#</sup>, Maria-Christina Zennaro<sup>1,2,3#</sup>

<sup>1</sup>INSERM, UMRS\_970, Paris Cardiovascular Research Center, Paris, France

<sup>2</sup>Université Paris Descartes, Sorbonne Paris Cité, Paris, France

<sup>3</sup>Assistance Publique-Hôpitaux de Paris, Hôpital Européen Georges Pompidou, Service de Génétique, Paris, France

<sup>4</sup>Leibniz-Forschungsinstitut für Molekulare Pharmakologie (FMP), Berlin, Germany

<sup>5</sup>Max-Delbrück-Centrum für Molekulare Medizin (MDC), Berlin, Germany

<sup>6</sup>Division of Pediatric Endocrinology, Department of Pediatrics, All India Institute of Medical Sciences, New Delhi, India

<sup>7</sup>Assistance Publique-Hôpitaux de Paris, Hôpital Européen Georges Pompidou, Unité Hypertension artérielle, Paris, France

<sup>8</sup>Normandie Univ, UNIROUEN, Rouen, France

<sup>9</sup>INSERM, DC2N, Rouen, France

<sup>10</sup>Department of Endocrinology, Diabetes and Metabolic Diseases, University Hospital of Rouen, Rouen, France

<sup>11</sup>Institute of Human Genetics, Helmholtz Zentrum München, Neuherberg, Germany

<sup>12</sup>Institute of Human Genetics, Technische Universität München, Munich, Germany

\*,<sup>S</sup>,<sup>^</sup> equal contribution

#Corresponding authors

Address correspondence to:

Maria-Christina Zennaro, MD, PhD

INSERM, U970

Paris Cardiovascular Research Center – PARCC

56, rue Leblanc,

75015 Paris – France

Tel : +33 (0)1 53 98 80 42

Fax : + 33 (0)1 53 98 79 52

e-mail : [maria-christina.zennaro@inserm.fr](mailto:maria-christina.zennaro@inserm.fr)

Fabio Fernandes Rosa, MD, PhD

INSERM, U970

Paris Cardiovascular Research Center – PARCC

56, rue Leblanc,

75015 Paris – France

Tel : +33 (0)1 53 98 80 43

Fax : + 33 (0)1 53 98 79 52

e-mail : [fabio.fernandes-rosa@inserm.fr](mailto:fabio.fernandes-rosa@inserm.fr)

Thomas J. Jentsch, MD, PhD

FMP / MDC

Robert-Rössle-Strasse 10

13125 Berlin – Germany

Tel: +49 30 9406 2961  
Fax: +49 30 9406 2960  
e-mail: [Jentsch@fmp-berlin.de](mailto:Jentsch@fmp-berlin.de)

## INTRODUCTORY PARAGRAPH

Primary aldosteronism is the most common and curable form of secondary arterial hypertension. We performed whole exome sequencing in patients with early-onset primary aldosteronism and identified a *de novo* heterozygous c.71G>A/p.Gly24Asp mutation in the *CLCN2* gene, coding for the voltage-gated ClC-2 chloride channel<sup>1</sup>, in a patient diagnosed at age 9 ys. Patch-clamp analysis of glomerulosa cells of mouse adrenal gland slices revealed hyperpolarization-activated Cl<sup>-</sup> currents that were abolished in *Clcn2*<sup>-/-</sup> mice. The p.Gly24Asp mutation, located in a well conserved ‘inactivation domain’<sup>2,3</sup>, abolished the voltage- and time-dependent gating of ClC-2 and strongly increased Cl<sup>-</sup> conductance at resting potentials. Expression of ClC-2<sub>24Asp</sub> in adrenocortical cells increased expression of aldosterone synthase and aldosterone production.

Our data indicate that *CLCN2* mutations cause primary aldosteronism. They highlight for the first time the important role of chloride in aldosterone biosynthesis and identify ClC-2 as the foremost chloride conductor of resting glomerulosa cells.

1           **MAIN TEXT**

2           Arterial hypertension is a major cardiovascular risk factor <sup>4</sup>. Primary aldosteronism is  
3 the most common and curable form of secondary arterial hypertension, with an estimated  
4 prevalence of ~10% in referred patients and 4% in primary care<sup>5</sup>, and up to 20% of patients  
5 with resistant hypertension <sup>6</sup>. Primary aldosteronism results from autonomous aldosterone  
6 production in the adrenal cortex <sup>7</sup>, caused in most cases by a unilateral aldosterone-producing  
7 adenoma or bilateral adrenal hyperplasia (BAH). It is diagnosed on the basis of hypertension  
8 associated with increased aldosterone to renin ratio and often hypokalemia <sup>8</sup>. Compared to  
9 essential hypertension, increased aldosterone levels in primary aldosteronism are associated  
10 with increased cardiovascular risk in particular coronary artery disease, heart failure, renal  
11 damage and stroke <sup>9,10</sup>.

12 Gain-of-function mutations in different genes, coding for cation channels (*KCNJ5* <sup>11</sup>,  
13 *CACNAID* <sup>12,13</sup>, *CACNAIH* <sup>14,15</sup>) and ATPases (*ATP1A1* and *ATP2B3*, <sup>12,16</sup>), regulating  
14 intracellular ion homeostasis and plasma membrane potential, have been described in  
15 aldosterone producing adenoma and familial forms of primary aldosteronism, but the  
16 pathophysiology of many cases is still unknown.

17 We performed whole exome sequencing on germline DNA from 12 patients with young onset  
18 hypertension and hyperaldosteronism diagnosed before age 25 ys. Two index cases were  
19 investigated together with their parents and unaffected sibling to search for *de novo* variants.  
20 A *de novo* germline *CLCN2* variant c.71G>A (NM\_004366; p.Gly24Asp) was identified in  
21 subject K1011-1, but not in her asymptomatic parents (K1011-3 and K1011-4) and sibling  
22 (K1011-2, Fig. 1a and 1b, Table 1). The variant was absent from more than 120.000 alleles in  
23 the Exome Aggregation Consortium (ExAC) and in our in-house database. We did not find  
24 additional *CLCN2* variants among the other 11 investigated individuals. *CLCN2* encodes the  
25 chloride channel ClC-2. The variant *CLCN2* p.Gly24Asp localizes to its N-terminal  
26 cytoplasmic domain (Fig. 1c, d). Gly24 is highly conserved in ClC-2 orthologs of species as  
27 distant as zebrafish and *Xenopus* (Fig. 1c).

28 The patient carrying the *CLCN2* p.Gly24Asp variant is a 9 year old girl, who presented  
29 with severe headache and vomiting lasting for 1 year (Table 1). The child was  
30 developmentally normal, first born to a non-consanguineous couple. There was history of  
31 mild hypertension in maternal grandmother and granduncle. Blood pressure (BP) was 172/100  
32 mm Hg, heart rate was 120/minute. The rest of the examination was normal. Her work-up  
33 revealed persistent hypokalemia (serum K<sup>+</sup> ranging from 1.8 to 2.4 meq/L), elevated serum  
34 aldosterone (868.1 pg/ml, reference range 12-340 pg/ml) and suppressed plasma renin activity  
35 (0.11 ng/ml/hr, reference range 1.9 to 6.0 ng/ml/hr in upright posture), suggestive of primary  
36 aldosteronism. Abdominal CT scan showed no adrenal abnormalities. Other parameters  
37 including 24 hours urinary vanillylmandelic acid and serum cortisol were normal.  
38 Hypertension was initially managed with amlodipin, enalapril and atenolol. Once the  
39 diagnosis of primary aldosteronism was made, spironolactone was added, enalapril was  
40 stopped and doses of amlodipin and atenolol were reduced. Serum K<sup>+</sup> normalized. A positive  
41 glucocorticoid suppression test (aldosterone 949.3 pg/ml at baseline and 56.9 pg/ml after

42 administration of oral dexamethasone 0.5 mg every 6 hours for 48 hours) suggested the  
43 possibility of glucocorticoid remediable aldosteronism (GRA), a rare familial form of  
44 hyperaldosteronism<sup>17</sup>. However, genetic analysis for a chimeric *CYP11B1/CYP11B2* gene  
45 was negative. The child's hypertension has been well controlled over the last 18 months with  
46 prednisolone 5mg/m<sup>2</sup>/day, spironolactone and amlodipin. On treatment, her serum aldosterone  
47 and plasma renin are 421 pg/ml (reference range 25 to 392) and 8.22 μU/mL (4.4 to 46.1).  
48 After exclusion of GRA by genetic testing, prednisolone treatment was stopped.

49 Cl<sup>-</sup> conductances can regulate the excitability of neuronal, muscle, and endocrine cells  
50<sup>18-21</sup>. In zona glomerulosa cells, ACTH-activated Cl<sup>-</sup> currents have been described<sup>22</sup>, but their  
51 outward rectification sets them apart from hyperpolarization-activated ClC-2 currents. ClC-2  
52 is expressed in almost all tissues<sup>1</sup> and may have roles in ion homeostasis and transepithelial  
53 transport<sup>23</sup>. *Clcn2*<sup>-/-</sup> mice display early postnatal retinal and testicular degeneration<sup>24</sup> as well  
54 as leukodystrophy<sup>25,26</sup>; in humans, *CLCN2* loss-of-function mutations result in  
55 leukodystrophy<sup>27</sup> that may be associated with azoospermia<sup>28</sup>. These phenotypes have been  
56 ascribed to a role of ClC-2 in extracellular ion homeostasis<sup>24,25</sup>.

57 Data retrieved from a transcriptome analysis including eleven human adrenals<sup>29</sup>  
58 showed high expression of *CLCN2* in human adrenal cortex (Supplementary Table 1). In  
59 mice, Western blots revealed similar expression of ClC-2 in whole adrenal gland as in brain  
60 (Fig. 2a), which expresses substantial, physiologically important amounts of ClC-2<sup>25</sup>. Patch-  
61 clamp analysis of glomerulosa cells *in situ* revealed typical hyperpolarization-activated  
62 currents in WT, but not in *Clcn2*<sup>-/-</sup> mice (Fig. 2 b,c). Their magnitude was similar to those  
63 observed in Bergmann glia which prominently express ClC-2<sup>26</sup>. The almost complete  
64 absence of Cl<sup>-</sup> currents in *Clcn2*<sup>-/-</sup> cells demonstrates that under resting conditions ClC-2  
65 mediates the bulk of glomerulosa cell Cl<sup>-</sup> currents.

66 The *CLCN2* p.Gly24Asp mutation is located in a highly conserved ‘inactivation  
67 domain’<sup>2,3</sup> of the channel. Deletions and point mutations in this region and an intracellular  
68 loop<sup>2</sup> (highlighted in Fig. 1c, d) lead to ‘open’ CIC-2 channels that have lost their sensitivity  
69 to voltage, cell swelling, or external pH<sup>2,3</sup>. Likewise, insertion of the p.Gly24Asp mutation  
70 drastically changed voltage-dependent gating of CIC-2 (Fig. 2d,e,h) and dramatically  
71 increased current amplitudes when expressed in *Xenopus* oocytes (Fig. 2d-g). When measured  
72 at -80 mV, the approximate resting potential of glomerulosa cells<sup>30</sup>, current amplitudes from  
73 the mutant channel were much larger compared to WT (Fig. 2d-f). Linear, ohmic currents like  
74 those of the mutant channel might be due to unspecific electrical leaks; however, currents of  
75 both WT and mutant CIC-2 were markedly reduced when extracellular chloride was replaced  
76 by iodide (Fig. 2d-f), agreeing with the Cl<sup>-</sup>>I<sup>-</sup> selectivity of CLC channels in general<sup>23</sup> and  
77 CIC-2 in particular<sup>1</sup>. The activation of CIC-2 by acid extracellular pH can be almost  
78 abolished by mutations in the ‘inactivation domain’<sup>2</sup>. Likewise, the CIC-2<sub>24Asp</sub> mutant had  
79 largely reduced pH sensitivity (Fig. 2i-j, Supplementary Fig.1). In conclusion, the  
80 p.Gly24Asp mutation results in a strong gain of function, explaining the dominant disease  
81 phenotype of the mutation that is present at the heterozygote state. It also suggests a  
82 pathophysiological mechanism in which a strong increase in Cl<sup>-</sup> currents may depolarize  
83 glomerulosa cells, thereby opening voltage-gated Ca<sup>2+</sup> channels and activating transcriptional  
84 programs via an increase of cytosolic Ca<sup>2+</sup>.

85 Expression of the mutant CIC-2<sub>24Asp</sub> channel in adrenocortical H295R-S2 cells, and  
86 conversely, knock-down of CIC-2 by shRNA significantly affected aldosterone production  
87 and expression of steroidogenic enzymes. Despite similar expression of CIC-2 in H295R-S2  
88 cells stably transfected with CIC-2<sub>24Asp</sub> or CIC-2<sub>WT</sub> (Fig. 3a and 3b), aldosterone synthase  
89 expression (Fig. 3a and 3c) and aldosterone production (Fig. 3d, e) were significantly  
90 increased in CIC-2<sub>24Asp</sub> expressing cells. Stimulation with angiotensin II (AngII 10nM) or K<sup>+</sup>

91 (12mM) increased aldosterone production in cells expressing WT CIC-2 (Fig. 3e). A further  
92 increase was observed in cells expressing CIC-2<sub>24Asp</sub> after AngII stimulation, but not after K<sup>+</sup>  
93 stimulation (Fig. 3e). Nevertheless, also after stimulation, aldosterone production in cells  
94 expressing CIC-2<sub>24Asp</sub> was significantly higher compared to cells expressing CIC-2<sub>WT</sub> (Fig.  
95 3e). Infection of H295R-S2 cells with CIC-2 shRNA reduced *CLCN2* expression by ~50%  
96 (Supplementary Fig. 2a) compared with a scrambled shRNA, and significantly reduced  
97 aldosterone production, both at baseline and after stimulation (Supplementary Fig. 2b),  
98 suggesting that even WT CIC-2 currents, although much smaller than currents from the  
99 Gly24Asp mutant, significantly increase the excitability of H295R-S2 adrenocortical cells.  
100 These changes were paralleled in both models by concomitant modifications of the expression  
101 of steroidogenic genes. A significant increase of mRNA expression of *CYP11B2* (encoding  
102 aldosterone synthase, Fig. 3f), *StAR* (encoding the Steroidogenic acute regulatory protein, Fig.  
103 3g) and *CYP21A2* (encoding Steroid 21-hydroxylase, Fig. 3h) was observed in CIC-2<sub>24Asp</sub>  
104 compared with CIC-2<sub>WT</sub> overexpressing cells in basal conditions. AngII increased expression  
105 of *StAR* and *CYP11B2*, while K<sup>+</sup> stimulation increased mRNA expression of *CYP11B2*.  
106 Conversely, knock-down of CIC-2 led to a significant decrease in *CYP11B2* expression in all  
107 conditions (Supplementary Fig. 2c). These data further support the notion that a gain-of-  
108 function *CLCN2* mutation may depolarize the cell, activate the steroidogenic pathway, and  
109 increase aldosterone production. While knock-down of CIC-2 influences aldosterone  
110 production in H295R-S2 cells which have a resting potential of about – 65 mV (Fig. 4a, b),  
111 this may not be the case in native glomerulosa cells. Because their V<sub>m</sub> is close to the K<sup>+</sup>  
112 equilibrium potential<sup>30</sup>, they are unlikely to markedly hyperpolarize upon loss of CIC-2. No  
113 changes of blood pressure have been reported for mice or patients lacking CIC-2<sup>24,25,27</sup>, but  
114 this issue has not been investigated in detail.

115 We next explored the effect of the ClC-2 Gly24Asp mutation on the membrane  
116 potential and on calcium influx through voltage-gated calcium channels. These studies were  
117 performed with the perforated patch clamp technique which does not disturb the intracellular  
118 chloride concentration and is required to see the full effect of 'inactivation domain'<sup>2,3</sup>  
119 mutations<sup>31,32</sup>. In the stably transfected H295R-S2 cells used to investigate steroidogenesis  
120 (Fig. 3), there was a trend of  $V_m$  to be depolarized in ClC-2<sub>24Asp</sub> transfected compared to ClC-  
121 2<sub>WT</sub> transfected cells (mean values of roughly -52 and -67 mV, respectively) (Fig. 4a).  
122 However, because these cell lines are not clonal, the variability was large and the difference  
123 was not statistically significant.

124 We therefore resorted to transient transfection of H295R-S2 cells which allowed us to  
125 select ClC-2 expressing cells by fluorescence of co-transfected GFP (Fig. 4b-g). Although  
126 these cells express ClC-2 less efficiently than *Xenopus* oocytes (compare Fig. 4f and 2d) and  
127 HEK cells<sup>31,32</sup>, ClC-2<sub>24Asp</sub> expressing cells displayed robust chloride currents that lacked  
128 strong voltage-dependence (Fig. 4c-g). The observed increase in currents may reflect both an  
129 increase in currents per channel and in the number of channels; both must be considered when  
130 analyzing pathogenic effects of ion channel mutants. This increase in currents correlated with a  
131 strong depolarization from  $V_m = -65 \pm 4$  (ClC-2<sub>WT</sub>) to  $-46 \pm 4$  mV in ClC-2<sub>24Asp</sub> transfected  
132 cells (Fig. 4b), indicating that chloride concentration in H295R-S2 cells is higher than  
133 predicted by the electrochemical equilibrium. This depolarization may open voltage-  
134 dependent calcium channels. Indeed, nifedipine (an L-type calcium channel blocker) and/or  
135 mibefradil (a T-type calcium channel blocker) strongly reduced aldosterone production in  
136 cells expressing the ClC-2<sub>24Asp</sub> mutant (Fig. 4i). The involvement of L-type calcium channels  
137 appeared to be larger in ClC-2<sub>24Asp</sub> expressing cells (Fig. 4h), possibly because of their  
138 depolarized plasma membrane potential which is required to open these channels<sup>33</sup>. However,

139 we cannot exclude that nifedipine acted partially through T-type calcium channels, which are  
140 also blocked by this compound at depolarized voltages<sup>34</sup>.

141 To investigate whether the *CLCN2* p.Gly24Asp mutation could be involved in other  
142 forms of primary aldosteronism, we sequenced exon 2 of *CLCN2* in 100 patients with BAH.  
143 While *CLCN2* p.Gly24Asp was not identified among these subjects, we identified two rare  
144 *CLCN2* variants, c.197G>A (p.Arg66Gln, rs755883734) and c.143C>G (p.Pro48Arg,  
145 rs115661422) in two subjects (Supplementary Fig. 3). Minor allele frequencies of these  
146 variants are very low in the ExAC database (*CLCN2* p.Arg66Gln 0.00003; *CLCN2*  
147 p.Pro48Arg 0.0017). Both variants failed to significantly change CIC-2 currents in  
148 heterologous expression (Supplementary Fig. 4), in spite of a previously described<sup>35</sup> moderate  
149 reduction of CIC-2<sub>Pro48Arg</sub> current amplitudes. Nonetheless, it is noteworthy that the two  
150 patients were diagnosed with hypertension at young age, 29 and 19 ys respectively (Table 1)  
151 and in both cases during pregnancy. Finally, sequencing the *CLCN2* exons encoding the N-  
152 terminal domain (exon 1 and 2) and the loop between helices J and K (exon 10),  
153 corresponding to the CIC-2 ‘inactivation domains’<sup>2,3</sup>, in 20 additional patients with  
154 hypertension before age 20 did not identify additional mutations. Among these patients, nine  
155 had a history of hypertension before the age of 15 years (one before age 10 ys), indicating that  
156 *CLCN2* mutations might underlie very young onset forms of primary aldosteronism.

157 In conclusion, we show that a gain-of-function mutation in the CIC-2 chloride channel  
158 underlies a genetic form of secondary arterial hypertension and identify CIC-2 as the foremost  
159 chloride conductor of resting glomerulosa cells. We suggest that increased Cl<sup>-</sup> currents  
160 induced by the CIC-2 p.Gly24Asp mutation could depolarize the zona glomerulosa cell  
161 membrane, thereby opening voltage-gated calcium channels which trigger autonomous  
162 aldosterone production by increasing intracellular Ca<sup>2+</sup> concentrations (Fig. 5b, red arrows).  
163 We hypothesize that the increased Cl<sup>-</sup> currents may overcome the hyperpolarizing currents of

164  $K^+$  channels that normally determine the glomerulosa cell resting potential. The inhibition of  
165 these potassium channels e.g. upon AngII stimulation, or the depolarizing currents mediated  
166 by these channels upon increases in extracellular  $K^+$ , are the main mechanisms triggering  
167 aldosterone production under physiological conditions (Fig. 5a, dashed black arrows).

168 Not only mutations in the amino-terminal CIC-2 'inactivation domain'<sup>2,3</sup>, like the  
169 Gly24Asp mutation found here, but also in the cytoplasmic linker between transmembrane  
170 helices J and K may cause primary aldosteronism (Fig. 1d). Several point mutations in that  
171 linker result in constitutively open CIC-2 channels<sup>2</sup>. We propose both regions as potential  
172 hotspots for mutations causing primary aldosteronism. The discovery that a chloride channel  
173 is involved in primary aldosteronism opens new and unexpected perspectives for the  
174 pathogenesis and treatment of arterial hypertension.

175

176 **Acknowledgements**

177 This work was funded through institutional support from INSERM and by the Agence  
178 Nationale pour la Recherche (ANR-13-ISV1-0006-01), the Fondation pour la Recherche  
179 Médicale (DEQ20140329556), the Programme Hospitalier de Recherche Clinique (PHRC  
180 grant AOM 06179), and by institutional grants from INSERM. The laboratory of Dr. Maria-  
181 Christina Zennaro is also partner of the H2020 project ENSAT-HT grant n° 633983. Thomas  
182 J. Jentsch was supported by institutional funding from the Leibniz and Helmholtz  
183 Associations, a grant from the BMBF (E-RARE 01GM1403) and by the Prix Louis-Jeantet de  
184 Médecine.

185

186 **Conflict of interest**

187 The authors have nothing to disclose.

188

189 **Author Contributions**

190 MCZ, FFR, GD, IJO and TJJ designed experiments and wrote the manuscript. TMS, MCZ,  
191 TS and FFR performed and analyzed whole exome sequencing. MCZ, FFR, GD, REZ and  
192 SB performed and analyzed *in vitro* studies on H295R-S2 cells. IJO performed  
193 electrophysiological studies that were analyzed by IJO and TJJ. CG characterized adrenal  
194 glands from WT and *Cln2*<sup>-/-</sup> mice and performed Western blots. VJ, XJ, LA, and HL were  
195 responsible for patients' recruitment, medical care and clinical data acquisition. All authors  
196 revised the manuscript draft.

197

198

199

200 **References**

- 201 1. Thiemann, A., Grunder, S., Pusch, M. & Jentsch, T.J. A chloride channel widely  
202 expressed in epithelial and non-epithelial cells. *Nature* **356**, 57-60 (1992).
- 203 2. Jordt, S.E. & Jentsch, T.J. Molecular dissection of gating in the CIC-2 chloride  
204 channel. *EMBO J.* **16**, 1582-92 (1997).
- 205 3. Grunder, S., Thiemann, A., Pusch, M. & Jentsch, T.J. Regions involved in the opening  
206 of CIC-2 chloride channel by voltage and cell volume. *Nature* **360**, 759-62 (1992).
- 207 4. Worldwide trends in blood pressure from 1975 to 2015: a pooled analysis of 1479  
208 population-based measurement studies with 19.1 million participants. *Lancet* **389**, 37-  
209 55 (2017).
- 210 5. Hannemann, A. & Wallaschofski, H. Prevalence of primary aldosteronism in patient's  
211 cohorts and in population-based studies--a review of the current literature. *Horm.*  
212 *Metab. Res.* **44**, 157-62 (2012).
- 213 6. Calhoun, D.A. Hyperaldosteronism as a common cause of resistant hypertension.  
214 *Annu. Rev. Med.* **64**, 233-47 (2013).
- 215 7. Zennaro, M.C., Boulkroun, S. & Fernandes-Rosa, F. Genetic Causes of Functional  
216 Adrenocortical Adenomas. *Endocr. Rev.* **38**, 516-537 (2017).
- 217 8. Funder, J.W. *et al.* The Management of Primary Aldosteronism: Case Detection,  
218 Diagnosis, and Treatment: An Endocrine Society Clinical Practice Guideline. *J. Clin.*  
219 *Endocrinol. Metab.* **101**, 1889-916 (2016).
- 220 9. Savard, S., Amar, L., Plouin, P.F. & Steichen, O. Cardiovascular complications  
221 associated with primary aldosteronism: a controlled cross-sectional study.  
222 *Hypertension* **62**, 331-6 (2013).
- 223 10. Rossi, G.P. *et al.* A prospective study of the prevalence of primary aldosteronism in  
224 1,125 hypertensive patients. *J. Am. Coll. Cardiol.* **48**, 2293-300 (2006).

- 225 11. Choi, M. *et al.* K<sup>+</sup> channel mutations in adrenal aldosterone-producing adenomas and  
226 hereditary hypertension. *Science* **331**, 768-72 (2011).
- 227 12. Azizan, E.A. *et al.* Somatic mutations in ATP1A1 and CACNA1D underlie a common  
228 subtype of adrenal hypertension. *Nat. Genet.* **45**, 1055-60 (2013).
- 229 13. Scholl, U.I. *et al.* Somatic and germline CACNA1D calcium channel mutations in  
230 aldosterone-producing adenomas and primary aldosteronism. *Nat. Genet.* **45**, 1050-4  
231 (2013).
- 232 14. Scholl, U.I. *et al.* Recurrent gain of function mutation in calcium channel CACNA1H  
233 causes early-onset hypertension with primary aldosteronism. *Elife* **4**, e06315 (2015).
- 234 15. Daniil, G. *et al.* CACNA1H Mutations Are Associated With Different Forms of  
235 Primary Aldosteronism. *EBioMedicine* **13**, 225-236 (2016).
- 236 16. Beuschlein, F. *et al.* Somatic mutations in ATP1A1 and ATP2B3 lead to aldosterone-  
237 producing adenomas and secondary hypertension. *Nat. Genet.* **45**, 440-4, 444e1-2  
238 (2013).
- 239 17. Lifton, R.P. *et al.* A chimaeric 11beta-hydroxylase aldosterone synthase gene causes  
240 glucocorticoid-remediable aldosteronism and human hypertension. *Nature* **355**, 262-  
241 265 (1992).
- 242 18. Moss, S.J. & Smart, T.G. Constructing inhibitory synapses. *Nat. Rev. Neurosci.* **2**,  
243 240-50 (2001).
- 244 19. Rinke, I., Artmann, J. & Stein, V. ClC-2 voltage-gated channels constitute part of the  
245 background conductance and assist chloride extrusion. *J. Neurosci.* **30**, 4776-86  
246 (2010).
- 247 20. Koch, M.C. *et al.* The skeletal muscle chloride channel in dominant and recessive  
248 human myotonia. *Science* **257**, 797-800 (1992).

- 249 21. Guo, J.H. *et al.* Glucose-induced electrical activities and insulin secretion in  
250 pancreatic islet beta-cells are modulated by CFTR. *Nat. Commun.* **5**, 4420 (2014).
- 251 22. Chorvatova, A., Gendron, L., Bilodeau, L., Gallo-Payet, N. & Payet, M.D. A Ras-  
252 dependent chloride current activated by adrenocorticotropin in rat adrenal zona  
253 glomerulosa cells. *Endocrinology* **141**, 684-92 (2000).
- 254 23. Jentsch, T.J. Discovery of CLC transport proteins: cloning, structure, function and  
255 pathophysiology. *J. Physiol.* **593**, 4091-109 (2015).
- 256 24. Bosl, M.R. *et al.* Male germ cells and photoreceptors, both dependent on close cell-  
257 cell interactions, degenerate upon CLC-2 Cl<sup>-</sup> channel disruption. *EMBO J.* **20**, 1289-  
258 99 (2001).
- 259 25. Blanz, J. *et al.* Leukoencephalopathy upon disruption of the chloride channel CLC-2. *J.*  
260 *Neurosci.* **27**, 6581-9 (2007).
- 261 26. Hoegg-Beiler, M.B. *et al.* Disrupting MLC1 and GlialCAM and CLC-2 interactions in  
262 leukodystrophy entails glial chloride channel dysfunction. *Nat. Commun.* **5**, 3475  
263 (2014).
- 264 27. Depienne, C. *et al.* Brain white matter oedema due to CLC-2 chloride channel  
265 deficiency: an observational analytical study. *Lancet Neurol.* **12**, 659-68 (2013).
- 266 28. Di Bella, D. *et al.* Subclinical leukodystrophy and infertility in a man with a novel  
267 homozygous CLCN2 mutation. *Neurology* **83**, 1217-8 (2014).
- 268 29. Boulkroun, S. *et al.* Prevalence, Clinical, and Molecular Correlates of KCNJ5  
269 Mutations in Primary Aldosteronism. *Hypertension* **59**, 592-8 (2012).
- 270 30. Spat, A. & Hunyady, L. Control of aldosterone secretion: a model for convergence in  
271 cellular signaling pathways. *Physiol. Rev.* **84**, 489-539 (2004).

- 272 31. Varela, D., Niemeyer, M.I., Cid, L.P. & Sepulveda, F.V. Effect of an N-terminus  
273 deletion on voltage-dependent gating of the ClC-2 chloride channel. *J. Physiol.* **544**,  
274 363-72 (2002).
- 275 32. Pusch, M., Jordt, S.E., Stein, V. & Jentsch, T.J. Chloride dependence of  
276 hyperpolarization-activated chloride channel gates. *J. Physiol.* **515 ( Pt 2)**, 341-53  
277 (1999).
- 278 33. Barrett, P.Q. *et al.* Role of voltage-gated calcium channels in the regulation of  
279 aldosterone production from zona glomerulosa cells of the adrenal cortex. *J. Physiol.*  
280 **594**, 5851-5860 (2016).
- 281 34. Perez-Reyes, E., Van Deusen, A.L. & Vitko, I. Molecular pharmacology of human  
282 Cav3.2 T-type Ca<sup>2+</sup> channels: block by antihypertensives, antiarrhythmics, and their  
283 analogs. *J. Pharmacol. Exp. Ther.* **328**, 621-7 (2009).
- 284 35. Paul, J. *et al.* Alterations in the cytoplasmic domain of CLCN2 result in altered gating  
285 kinetics. *Cell. Physiol. Biochem.* **20**, 441-54 (2007).
- 286 36. Dutzler, R., Campbell, E.B., Cadene, M., Chait, B.T. & MacKinnon, R. X-ray  
287 structure of a ClC chloride channel at 3.0 Å reveals the molecular basis of anion  
288 selectivity. *Nature* **415**, 287-94 (2002).

289

290

291

292 **FIGURE LEGENDS**

293 **Figure 1. A *CLCN2* variant identified in a patient with early onset primary**  
294 **aldosteronism.** (a) Pedigree of kindred K1011. The subject with PA is shown with a black  
295 symbol and non-affected subjects are shown with white symbols. (b) Sanger sequencing  
296 chromatograms showing the *CLCN2* wild-type sequence of the unaffected parents (K1011-3  
297 and K1011-4) and brother (K1011-2) and the *CLCN2* variant c.71G>A (p.Gly24Asp)  
298 identified in the patient with early onset primary aldosteronism (K1011-1). (c) Alignment and  
299 conservation of residues encoded by *CLCN2* orthologs. The red box indicates the amino-  
300 terminal 'inactivation domain' of CIC-2. Several deletions and mutations in this region of rat  
301 CIC-2 led to constitutive open CIC-2 channels (uninterrupted line) or partially opened  
302 channels (dashed line) <sup>3</sup>. Residues that are conserved among more than 3 sequences are  
303 highlighted in yellow. (d) Position of the disease-causing Gly24Asp mutation in the CIC-2  
304 protein (schematic transmembrane topology drawing modified from <sup>36</sup>). 'Inactivation  
305 domains' previously identified by structure-function analysis in the amino-terminus <sup>3</sup> and an  
306 intracellular loop <sup>2</sup> of CIC-2 are shown in red. Several point mutations and deletions in these  
307 domains open the CIC-2 channel <sup>2,3</sup> similar to the Gly24Asp substitution described here.  
308 CBS1 and CBS2, cystathionine- $\beta$ -synthase domains which can affect gating of CLC channels  
309 <sup>23</sup>.

310 **Figure 2 CIC-2 expression in mouse adrenals and electrophysiological analyses of WT**  
311 **and mutant channels.** (a) CIC-2 immunoblot of brain and adrenals from *Clcn2*<sup>+/+</sup> and *Clcn2*  
312 <sup>-/-</sup> mice. All lanes are from the same blot, which has been cut as indicated. Similar amounts of  
313 protein were loaded with actin serving as loading control. This blot is representative for three  
314 independent experiments. (b) Representative whole-cell chloride current traces of mouse zona  
315 glomerulosa cells from *Clcn2*<sup>+/+</sup> (top) and *Clcn2*<sup>-/-</sup> (bottom) adrenal slices using voltage steps  
316 as indicated above. (c) Mean  $\pm$  SEM currents measured after 1.5 s from experiments in (b)

317 plotted as a function of clamp voltage. (d, e) Representative chloride current traces measured  
318 by two-electrode voltage-clamp from *Xenopus* oocytes injected with either human CIC-2<sub>WT</sub>  
319 (d) or CIC-2<sub>24Asp</sub> (e) cRNA, using the protocol shown in (d). For some measurements (below)  
320 extracellular chloride was replaced with iodide. (f) Mean  $\pm$  SEM currents measured in (d,e)  
321 plotted as a function of voltage. Number of cells indicated in parenthesis. (g, h) Summary of  
322 Cl<sup>-</sup> currents at -80 mV ( $I_{-80mV}$ ) (g) and current ratios ( $I_{-120mV} / I_{+60mV}$ ) as measure of  
323 rectification (h) (always measured at 2s) for panels (d-f). \*\*\*\*p < 0.0001, Mann-Whitney  
324 two-tailed test. (i, j) Effect of external pH on currents mediated by CIC-2<sub>WT</sub> (i) or CIC-2<sub>24Asp</sub>  
325 (j) in *Xenopus* oocytes. Currents were normalized to mean currents from respective construct  
326 measured after 2s at -120 mV and pH 7.4. Number of oocytes indicated in parenthesis, error  
327 bars indicate SEM.

328 **Figure 3. Effect of CIC-2<sub>WT</sub> and mutant CIC-2<sub>24Asp</sub> channels on aldosterone production**  
329 **and expression of genes and proteins involved in aldosterone biosynthesis.** (a) Western  
330 blots for CIC-2 and aldosterone synthase of H295R-S2 cells stably transfected with CIC-2<sub>WT</sub>  
331 or mutant CIC-2<sub>24Asp</sub>. These blots are representative of three independent experiments, with  
332 actin serving as loading control. (b) Quantification of CIC-2 protein expression in CIC-2<sub>WT</sub>  
333 and CIC-2<sub>24Asp</sub> H295R-S2 cells (T test p=0.10, F=3.19). (c) Quantification of aldosterone  
334 synthase expression in CIC-2<sub>WT</sub> or CIC-2<sub>24Asp</sub> H295R-S2 cells (T test p=0.0025, F=136). (d)  
335 Basal aldosterone production by H295R-S2 cells transfected with CIC-2<sub>WT</sub> or mutant CIC-  
336 2<sub>24Asp</sub> (T test, p=0.0008, F=142). (e) Basal and stimulated aldosterone production by H295R-  
337 S2 cells transfected with CIC-2<sub>WT</sub> (open bars) or mutant CIC-2<sub>24Asp</sub> (filled bars) (1way  
338 ANOVA p<0.0001, F=23.46). (f-h) Basal and stimulated mRNA expression of (f) *CYP11B2*  
339 (1way ANOVA p<0.001, F=18.39), (g) *STAR* (Kruskal-Wallis p=0.0033), and (h) *CYP21A2*  
340 (1way ANOVA p<0.0001, F23.27) in H295R-S2 cells transfected with CIC-2<sub>WT</sub> (open bars) or

341 mutant CIC-2<sub>24Asp</sub> (filled bars). Quantification of protein expression (using actin as loading  
342 control) and aldosterone production are represented as percentage of CIC-2<sub>WT</sub> in basal  
343 conditions and results of mRNA expression are represented as fold induction of CIC-2<sub>WT</sub> in  
344 basal conditions. Values of all experiments are represented as mean  $\pm$  SEM of three  
345 independent experiments performed in experimental triplicates (n=9) for each condition. \*  
346 p<0.05; \*\* p<0.01; \*\*\* p<0.001; i) p<0.05 stimulated vs basal condition, ii) p<0.01  
347 stimulated vs basal condition; iii) p<0.001 stimulated vs basal condition.

348 **Figure 4 Functional impact of the CIC-2<sub>24Asp</sub> mutation.** (a-g) Effect on membrane  
349 potential  $V_m$  and plasma membrane anion currents in H295R-S2 cells. (a) Resting membrane  
350 potential of CIC-2<sub>WT</sub> and CIC-2<sub>24Asp</sub> stably transfected H295R-S2 cells which were used to  
351 determine aldosterone secretion. Note strong mean depolarization (CIC-2<sub>WT</sub>,  $-67 \pm 2$  mV  
352 (n=8); CIC-2<sub>24Asp</sub>,  $-52 \pm 6$  mV (n=12)), which, however, was not significant (Two-tailed  
353 Mann-Whitney p = 0.14) owing to large variability of  $V_m$  of CIC-2<sub>24Asp</sub> transfected cells that  
354 were not cloned. (b) Similarly determined values of  $V_m$  for non-transfected, and transiently  
355 transfected H295R-S2 cells (non-transfected,  $-65 \pm 4$  mV (n=8); CIC-2<sub>WT</sub>,  $-69 \pm 7$  mV (n=4);  
356 CIC-2<sub>24Asp</sub>,  $-46 \pm 4$  mV (n=6); \*\*, Two-tailed Mann-Whitney p = 0.0095)) (c,d)  
357 Corresponding plasma membrane currents measured after 1.5 s under conditions eliminating  
358 cation inward currents as function of voltage (c) or as plot of individual values at  
359 physiological  $V_m$  of glomerulosa cells (d) \*, Two-tailed Mann-Whitney p = 0.019. (e-g)  
360 corresponding averaged current traces with 20 mV voltage steps between 0 and -120 mV. (h-i)  
361 Effect of calcium channel blockers on aldosterone production in H295R-S2 cells expressing  
362 (h) CIC-2<sub>WT</sub> (Kruskal Wallis p=0.0005) and (i) CIC-2<sub>24Asp</sub> (Kruskal Wallis, p=0.0032). Values  
363 represent mean  $\pm$  SEM of two independent experiments performed in experimental triplicates  
364 (n=6) for each condition. \* p<0.05; \*\* p<0.01.

365

366 **Figure 5. Proposed model for autonomous aldosterone secretion in adrenal zona**

367 **glomerulosa cells with the CIC-2<sub>24Asp</sub> mutation.** (a) In unstimulated conditions, the ZG cell

368 membrane potential closely follows the potassium resting potential at approximately -80 mV.

369 Increasing extracellular K<sup>+</sup> concentration, or inhibition of K<sup>+</sup> channels by AngII through its

370 receptor (AT1R), leads to cell membrane depolarization, opening of voltage-gated Ca<sup>2+</sup>

371 channels, and increased intracellular calcium concentrations, the major trigger for aldosterone

372 biosynthesis. Binding of AngII to AT1R also leads to G<sub>αq</sub>-mediated signaling and IP<sub>3</sub>-

373 mediated release of Ca<sup>2+</sup> from the endoplasmic reticulum. (b) The CIC-2 p.Gly24Asn

374 mutation abolishes the voltage-dependent gating of CIC-2. The resulting pronounced increase

375 of Cl<sup>-</sup> currents at resting potentials is proposed to result in cell depolarization, opening of

376 voltage gated Ca<sup>2+</sup> channel, stimulation of Ca<sup>2+</sup> signaling, and finally increased expression of

377 steroidogenic genes and aldosterone production.

378

379 **Table 1. Clinical and biological characteristics of patients carriers of *CLCN2* variants.**

	<b>K1011-1</b>	<b>K963-1</b>	<b>K1044-1</b>
<b>Sex</b>	F	F	F
<b>Age at HTN dg (ys)</b>	9	19	29
<b>Age at primary aldosteronism dg (ys)</b>	9	27	48
<b>SBP at primary aldosteronism dg (mmHg)</b>	172	139	173
<b>DBP at primary aldosteronism dg (mmHg)</b>	100	90	114
<b>Lowest plasma K<sup>+</sup> (mmol/L)</b>	1.8	2.9	2.5
<b>Urinary aldosterone (nmol/24h)</b>	ND	60	ND
<b>Plasma aldosterone (pmol/L)<sup>a</sup></b>	2406	927	1061
<b>Plasma renin (mU/L)<sup>a</sup></b>	0.9	1.9	<1
<b>ARR (pmol/mU)<sup>b</sup></b>	481.2	185.4	212.2
<b>Adrenal abnormalities on imaging</b>	No	No	No
<b>Lateralization at AVS</b>	ND	No	No

380 dg, diagnosis; m, months; y, years ; HTN, hypertension; SBP, systolic blood pressure; DBP, diastolic  
381 blood pressure; K, potassium; ARR, aldosterone to renin ratio; Hormonal data are at diagnosis of  
382 primary aldosteronism. ND, not determined. For comparison within this table, plasma aldosterone  
383 levels for patient K1011-1 have been converted to pmol/L and plasma renin activity to plasma renin  
384 concentration. <sup>b</sup>for ARR calculation, renin values <5 have been transformed to 5. Conversion factor  
385 used for plasma aldosterone: 1 ng/l = 2.77 pmol/L; conversion factor used for plasma renin: 1 ng/ml/h  
386 = 8.2 mU/L.

387

388 **Online Methods**

389 ***Patients***

390 Patients with primary aldosteronism were recruited within the COMETE (Cortico- et  
391 MEdullo-surrénale, les Tumeurs Endocrines) network (COMETE-HEGP protocol,  
392 authorization CPP 2012-A00508-35) or in the context of genetic screening for familial  
393 hyperaldosteronism at the Genetics department of the HEGP. Methods for screening and  
394 subtype identification of primary aldosteronism were performed according to the Endocrine  
395 Society guidelines<sup>8</sup>. In patients diagnosed with primary aldosteronism, a thin slice CT scan or  
396 MRI of the adrenal and/or an adrenal venous sampling (AVS) were performed to differentiate  
397 between unilateral and bilateral aldosterone hypersecretion. All patients gave written  
398 informed consent for genetic and clinical investigation. Procedures were in accordance with  
399 institutional guidelines.

400

401 ***DNA isolation***

402 DNA from peripheral blood leukocytes was extracted using QIAamp DNA midi kit (Qiagen,  
403 Courtaboeuf Cedex, France) or salt-extraction.

404

405 ***Whole exome sequencing and variant detection***

406 Exomes were enriched in solution and indexed with SureSelect XT Human All Exon 50 Mb  
407 kits (Agilent). Sequencing was performed as 100 bp paired-end runs on HiSeq2000 systems  
408 (Illumina). Pools of 12 indexed libraries were sequenced on four lanes. Image analysis and  
409 base calling was performed using Illumina Real Time Analysis. CASAVA 1.8 was used for  
410 demultiplexing. BWA (v 0.5.9) with standard parameters was used for read alignment against  
411 the human genome assembly hg19 (GRCh37). We performed single-nucleotide variant and  
412 small insertion and deletion (indel) calling specifically for the regions targeted by the exome

413 enrichment kit, using SAMtools (v 0.1.18). Subsequently the variant quality was determined  
414 using the SAMtools varFilter script. We used default parameters, with the exception of the  
415 maximum read depth (-D) and the minimum P-value for base quality bias (-2), which we set  
416 to 9999 and 1e-400, respectively. Additionally, we applied a custom script to mark all  
417 variants with adjacent bases of low median base quality. All variants were then annotated  
418 using custom Perl scripts. Software is available on request (<https://ihg4.helmholtz->  
419 [muenchen.de/cgi-bin/mysql/snv-vcf/login.pl](https://ihg4.helmholtz-muenchen.de/cgi-bin/mysql/snv-vcf/login.pl)). Annotation included information about known  
420 transcripts (UCSC Known Genes and RefSeq genes), known variants (dbSNP v 135), type of  
421 mutation, and - if applicable – amino acid change in the corresponding protein. The annotated  
422 variants were then inserted into our in-house database. To reduce false positives we filtered  
423 out variants that were already present in our database, had variant quality less than 40, or  
424 failed one of the filters from the filter scripts. We then manually investigated the raw read  
425 data of the remaining variants using the Integrative Genomics Viewer (IGV).  
426

427 ***Sanger sequencing***

428 *CLCN2* DNA was amplified using the intron-spanning primers described in supplementary  
429 table S2. PCR were performed on 100 ng of DNA in a final volume of 25  $\mu$ l containing 0.75  
430 mM MgCl<sub>2</sub>, 400 nM of each primer, 200  $\mu$ M deoxynucleotide triphosphate, and 1.25 U Taq  
431 DNA Polymerase (Sigma). Cycling conditions for *CLCN2* were as previously described<sup>37</sup>  
432 with an annealing temperature of 60°C. Direct sequencing of PCR products was performed  
433 using the ABI Prism Big Dye Terminator® v3.1 Cycle Sequencing Kit (Applied Biosystems,  
434 Foster City, CA) on an ABI Prism 3700 DNA Analyzer (Applied Biosystems).

435

436 ***Site directed mutagenesis***

437 The CIC-2<sub>24Asp</sub> construct was generated by site-directed mutagenesis using the QuikChange II  
438 XL site-directed mutagenesis kit (Agilent). The mutation was introduced into the human CIC-  
439 2 cDNA fragment inserted into the pFROG expression vector<sup>38</sup> and their presence confirmed  
440 by Sanger sequencing.

441

442 ***Western blot***

443 The membrane fractions of tissue homogenate from brain and adrenal gland of adult *Clcn2*<sup>+/+</sup>  
444 and *Clcn2*<sup>-/-</sup> mice were isolated and lysed in 50mM Tris pH 6.8, 140mM NaCl, 0.5mM  
445 EDTA and 2% SDS with protease inhibitors (4 mM Pefabloc and Complete® EDTA-free  
446 protease inhibitor cocktail, Roche). Equal amounts of protein were separated by SDS-PAGE  
447 (10 % polyacrylamide) and blotted onto nitrocellulose. Rabbit polyclonal antibodies against a  
448 modified carboxy-terminal CIC-2 peptide have been described previously<sup>26</sup>. Blots were  
449 reprobed with mouse anti- $\beta$ -actin (Clone AC-74, Sigma A2228, 1:1000) as a loading control.  
450 H295R-S2 cells were lysed using RIPA buffer (Bio Basic Canada Inc.) with protease and  
451 phosphatase inhibitors mini tablets, EDTA free (Thermo Scientific). Proteins were solubilized

452 for 30 min at 4°C, under end-over-end rotation, and then centrifuged at 13000 rpm for 15 min  
453 at 4°C. Equal amounts of proteins were submitted to 10% SDS-PAGE and transferred onto  
454 nitrocellulose membrane. Membranes were blotted with rabbit anti-CIC-2 antibody (1:500),  
455 mouse anti-aldosterone synthase antibody (1:500, clone CYP11B2-41-13, kindly provided by  
456 Dr C Gomez Sanchez<sup>39</sup>) and mouse anti-β-actin (A2228, 1:10000, Sigma).

457

458

### 459 *Electrophysiological recordings*

460 Patch clamp analysis were performed in adrenal sections from wild type and *Cicn2*<sup>-/-</sup> mice<sup>24</sup>,  
461 similarly to previously described<sup>40</sup>. Bicarbonate based buffers were used which were  
462 continuously bubbled with 95% O<sub>2</sub> and 5% CO<sub>2</sub>. Briefly, adrenal glands were removed and  
463 placed into cold low-Ca<sup>2+</sup> solution composed of (in mM): 140 NaCl, 2 KCl, 26 NaHCO<sub>3</sub>, 10  
464 glucose, 5 MgCl<sub>2</sub>, 0.1 CaCl<sub>2</sub>, pH 7.4. The adrenals, after removal of surrounding fat tissue,  
465 were embedded in 3% low-melting agarose, sectioned at 70 μm (Leica VT1200S), and  
466 incubated at room temperature in solution containing: 140 NaCl, 2 KCl, 26 NaHCO<sub>3</sub>, 10  
467 glucose, 2 MgCl<sub>2</sub>, 2 CaCl<sub>2</sub>, and adjusted to pH 7.4. After at least 1 hour, slices were then  
468 transferred to a recording chamber and imaged with a 60x objective and DIC optics (Olympus  
469 BX51WI). Cells of the zona glomerulosa were identified by their rosette organization.  
470 Electrical signals were acquired at room temperature using a microelectrode amplifier  
471 (Multiclamp 700B) and software (Clampex 10.3, Molecular Devices, USA). As expected,  
472 cells when patched with a K<sup>+</sup>-based solution displayed spontaneous spiking which could be  
473 stimulated with angiotensin II. For measuring chloride currents, patch pipettes were filled  
474 with solution containing: 117.5 CsMeSO<sub>3</sub>, 17.5 CsCl, 4 NaCl, 10 Hepes, 1 EGTA, 1 MgCl<sub>2</sub>,  
475 adjusted to pH 7.3 while the bath solution contained: 117 NMDG-Cl, 23 NMDG-HCO<sub>3</sub>, 5  
476 CsCl, 1.3 MgCl<sub>2</sub>, 9 glucose, 2 CaCl<sub>2</sub>, adjusted to pH 7.3. Voltage steps from +40 to -120 mV

477 from a holding potential of  $-10$  mV were used, with a final 1 s step at  $+40$  mV. Signals were  
478 digitized at 10 kHz, filtered at 2 kHz and stored off-line for analysis with Clampfit software  
479 10.4.

480 For two electrode voltage clamp in *Xenopus laevis* oocytes, human wildtype and Gly24Asp  
481 CIC-2 cRNAs were prepared from pFROG vectors (Ambion mMACHINE mMACHINE T7  
482 kit) and injected into *X. laevis* oocytes, 13.8 ng and 9.2 ng per cell, respectively. Following  
483 two days of expression at  $17^{\circ}\text{C}$ , two electrode voltage clamp was performed at room  
484 temperature using a TurboTEC amplifier (npi electronic GmbH, Tamm, Germany) and  
485 pClamp Software (Molecular Devices) to elicit CIC-2 currents (2s steps from  $+60$ mV to -  
486  $120$ mV with a final 1s step at  $+40$ mV) in ND109 solution containing (in mM): 109 NaCl, 2  
487 KCl, 1 MgCl<sub>2</sub>, 1.8 CaCl<sub>2</sub>, 2 HEPES and adjusted to pH 7.4. To test for the typical Cl<sup>-</sup>>I<sup>-</sup>  
488 selectivity of CLC channels, currents were sequentially measured in solutions containing 109  
489 mM Cl<sup>-</sup> or 109 mM I<sup>-</sup>. To determine the pH sensitivity of currents, ND109 was buffered with  
490 5 mM MES for pH 6.5 and with 5 mM Tris for pH 8.5. Off-line analysis was performed with  
491 Clampfit software 10.4. Statistical significance was assessed using the Mann–Whitney test  
492 (Prism, GraphPad Software, USA).

493 For patch clamp of transiently transfected H295R-S2 cells, cells were seeded at 30%  
494 confluency onto poly-L-lysine (Sigma) coated glass coverslips. Once adhered they were  
495 transfected (X-fect) with bicistronic plasmids encoding emGFP (for identification of  
496 transfected cells) and, after an IRES sequence, CIC-2<sub>WT</sub> or CIC-2<sub>G24D</sub>. Cells were  
497 measured 12-24 hours later. Both transiently and stably transfected cells were measured  
498 using a Multiclamp 700B (Axon Instruments) amplifier Gramicidin-perforated patch clamp  
499 was performed to retain the intracellular chloride concentration. The tips of patch pipettes  
500 were first filled with gramicidin-free internal pipette solution (in mM): 100 KMeSO<sub>3</sub>, 30 KCl,  
501 4 NaCl, 10 Hepes, 1 MgCl<sub>2</sub>, 1 EGTA, 3 MgATP (pH 7.3, 280 mOsm/L) and then back-filled

502 with the same solution containing 25µg/mL gramicidin. GFP expressing cells were selected  
503 for analysis. Approximately 20 minutes following tight giga-seal formation, stable membrane  
504 potential measurements (I=0 configuration) could be acquired with access resistances of <100  
505 MΩ in bath solution containing 140 NaCl, 5 KCl, 10 Hepes, 1.8 MgCl<sub>2</sub>, 1.8 CaCl<sub>2</sub> (pH 7.4,  
506 300 mOsm/L). When adequate access resistance was attained (<35 MΩ), a Na<sup>+</sup>- and K<sup>+</sup>-free  
507 bath solution containing 140 CsCl, 10 Hepes, 1.8 MgCl<sub>2</sub>, 1.8 CaCl<sub>2</sub>, 20 sucrose (pH 7.3, 300  
508 mOsm/L) was perfused to measure anion membrane currents in the voltage clamp  
509 configuration (1s steps from +60 mV to -120 mV from a holding clamp of -10 mV).  
510 Measurements were performed at room temperature (22-24°C). Data are presented as mean  
511 ± SEM.

512

### 513 *Functional studies in H295R-S2 cells*

514 The human adrenocortical carcinoma cell line H295R strain 2 (H295R-S2), kindly  
515 provided by W. E. Rainey<sup>41</sup> was cultured in DMEM/Eagle's F12 medium (GIBCO, Life  
516 technologies, Carlsbad, CA) supplemented with 2% Ultrosor G (PALL life sciences, France),  
517 1% insulin/transferrin/selenium Premix (GIBCO, Life technologies, Carlsbad, CA), 10mM  
518 HEPES (GIBCO, Life technologies, Carlsbad, CA), 1% penicillin, and streptomycin (GIBCO,  
519 Life technologies, Carlsbad, CA) and maintained in a 37°C humidified atmosphere (5%  
520 CO<sub>2</sub>).

521 For overexpression experiments, H295R-S2 cells were seeded into tissue culture dishes 100 in  
522 groups of 5.000.000 cells per dish, and maintained in the conditions described. After 24h,  
523 cells were resuspended in 100 µl Nucleofector R solution (AMAXA kit, Lonza) and  
524 transfected with 3 µg of the ClC-2<sub>WT</sub> or ClC-2<sub>24Asp</sub> pFROG construct or a GFP construct,  
525 using the electroporation program P-20. To select only stably transfected cells, 48h post  
526 transfection cells were changed to medium containing 500 µg/mL G418-Genetycin (Gibco)

527 and used after all GFP transfected cells were dead. G418 selection was kept during all  
528 functional studies. For aldosterone measurements and RNA extraction, cells were serum  
529 deprived in DMEM/F12 containing 0.1% Ultrosor G for 24h and then incubated for another  
530 24h with fresh medium containing 0.1% Ultrosor G with no secretagogue or vehicle (basal),  
531 or secretagogues AngII (10nM) or  $K^+$  (12mM), or calcium channel blockers Nifedipine (L-  
532 Type calcium channel blocker, 10 $\mu$ M, Sigma) or Mibefradil (T-type calcium channel  
533 blocker, 10 $\mu$ M, Sigma). At the end of the incubation time, supernatant and cells from each  
534 well were harvested for aldosterone measurement and RNA extraction. Three experiments  
535 using aldosterone secretagogues (n=9) and two experiments using calcium channel blockers  
536 (n=6) were independently conducted in triplicate.

537 Human CIC2-targeting (TRCN0000427876) and non-mammalian control (SHC002V)  
538 MISSION shRNA lentiviral transduction particles were obtained from Sigma-Aldrich. The  
539 shRNA sequences were inserted into TRC2 pLKO-puro plasmid backbone. For the lentiviral  
540 infections, manufacturer's protocol was followed with slight modifications.  $1 \times 10^4$  H295R-S2  
541 cells were seeded in a 96-well plate. After 24 hours, medium was changed and supplemented  
542 with 2  $\mu$ g/ml polybrene (Sigma). Lentiviral particles were then added at a multiplicity of  
543 infection of 10 and medium changed after overnight incubation. For selection, 2  $\mu$ g/ml  
544 puromycin (Gibco) was added to the medium. After two passages cells were characterized in  
545 terms of mRNA expression and aldosterone production after incubation with or without  
546 secretagogue as mentioned above.

547

#### 548 ***RNA extraction and RT-qPCR***

549 Total RNA was extracted in Trizol reagent (Ambion Life technologies, Carlsbad CA)  
550 according to the manufacturer's recommendations. After deoxyribonuclease I treatment (Life  
551 Technologies, Carlsbad, CA), 500 ng of total RNA were retrotranscribed (iScript reverse

552 transcriptase, Biorad, Hercules, CA). Primers used for qPCR are described in supplementary  
553 table 3. The quantitative PCR was performed using SYBRgreen (Sso advanced universal  
554 SyBr Green supermix, Biorad, Hercules, CA) on a C1000 touch thermal cycler of Biorad  
555 (CFX96 Real Time System), according to the manufacturer's instructions. Controls without  
556 template were included to verify that fluorescence was not overestimated from primer dimer  
557 formation or PCR contaminations. RT-qPCR products were analyzed in a post amplification  
558 fusion curve to ensure that a single amplicon was obtained. Normalization for RNA quantity,  
559 and reverse transcriptase efficiency was performed against three reference genes (geometric  
560 mean of the expression of Ribosomal *18S* RNA, *HPRT*, and *GAPDH*), in accordance with the  
561 MIQE guidelines <sup>42</sup>. Quantification was performed using the standard curve method. Standard  
562 curves were generated using serial dilutions from a cDNA pool of all samples of each  
563 experiment, yielding a correlation coefficient of at least 0.98 in all experiments.

564

#### 565 *Aldosterone and protein assays*

566 Aldosterone levels were measured in cell culture supernatants by ELISA. Aldosterone  
567 antibody and aldosterone-3-CMO-biotin were kindly provided by Dr Gomez-Sanchez <sup>43</sup>.  
568 Aldosterone concentrations were normalized to cell protein concentrations (determined using  
569 Bradford protein assay).

570

#### 571 *Statistical analyses*

572 Quantitative variables are reported as means  $\pm$  standard error of the mean (SEM) when  
573 Gaussian distribution or medians and interquartile range when no Gaussian distribution.  
574 Pairwise comparisons were done with unpaired t-test or Mann-Whitney test respectively;  
575 multiple comparisons were done with the ANOVA test followed by a test for pairwise  
576 comparison of subgroups according to Bonferroni when Gaussian distribution, or Kruskal-

577 Wallis followed by Dunn's test when no Gaussian distribution. Comparisons between two  
578 groups were performed with two-tailed T test or two-tailed Mann-Whitney test. A p value <  
579 0.05 was considered significant. For functional experiments, all results were expressed as  
580 mean  $\pm$  SEM of three separate experiments performed in triplicate for CIC-2 overexpression  
581 studies with secretagogues, two separate experiments performed in triplicate for CIC-2  
582 expression studies with calcium channel blockers, and two to four separate experiments  
583 performed in triplicate for CIC-2 knockdown studies. Analyses were performed using Prism5  
584 (GraphPad software Inc, San Diego, CA).

585

#### 586 **Data availability.**

587 The data that support the findings of this study are available from the authors on reasonable  
588 request, see author contributions for specific data sets. Disease-causing variants have been  
589 submitted to ClinVar. Exome data are available on request within a scientific cooperation.

#### 590 **Online Methods References**

- 591 37. Hubert, E.L. *et al.* Mineralocorticoid receptor mutations and a severe recessive  
592 pseudohypoaldosteronism type 1. *J. Am. Soc. Nephrol.* **22**, 1997-2003 (2011).
- 593 38. Gunther, W., Luchow, A., Cluzeaud, F., Vandewalle, A. & Jentsch, T.J. CIC-5, the  
594 chloride channel mutated in Dent's disease, colocalizes with the proton pump in  
595 endocytotically active kidney cells. *Proc. Natl. Acad. Sci. U S A* **95**, 8075-80 (1998).
- 596 39. Gomez-Sanchez, C.E. *et al.* Development of monoclonal antibodies against human  
597 CYP11B1 and CYP11B2. *Mol. Cell. Endocrinol.* **383**, 111-7 (2014).
- 598 40. Hu, C., Rusin, C.G., Tan, Z., Guagliardo, N.A. & Barrett, P.Q. Zona glomerulosa cells  
599 of the mouse adrenal cortex are intrinsic electrical oscillators. *J. Clin. Invest.* **122**,  
600 2046-53 (2012).

- 601 41. Wang, T. *et al.* Comparison of aldosterone production among human adrenocortical  
602 cell lines. *Horm. Metab. Res.* **44**, 245-50 (2012).
- 603 42. Bustin, S.A. *et al.* The MIQE guidelines: minimum information for publication of  
604 quantitative real-time PCR experiments. *Clin. Chem.* **55**, 611-22 (2009).
- 605 43. Gomez-Sanchez, C.E. *et al.* The production of monoclonal antibodies against  
606 aldosterone. *Steroids* **49**, 581-7 (1987).
- 607

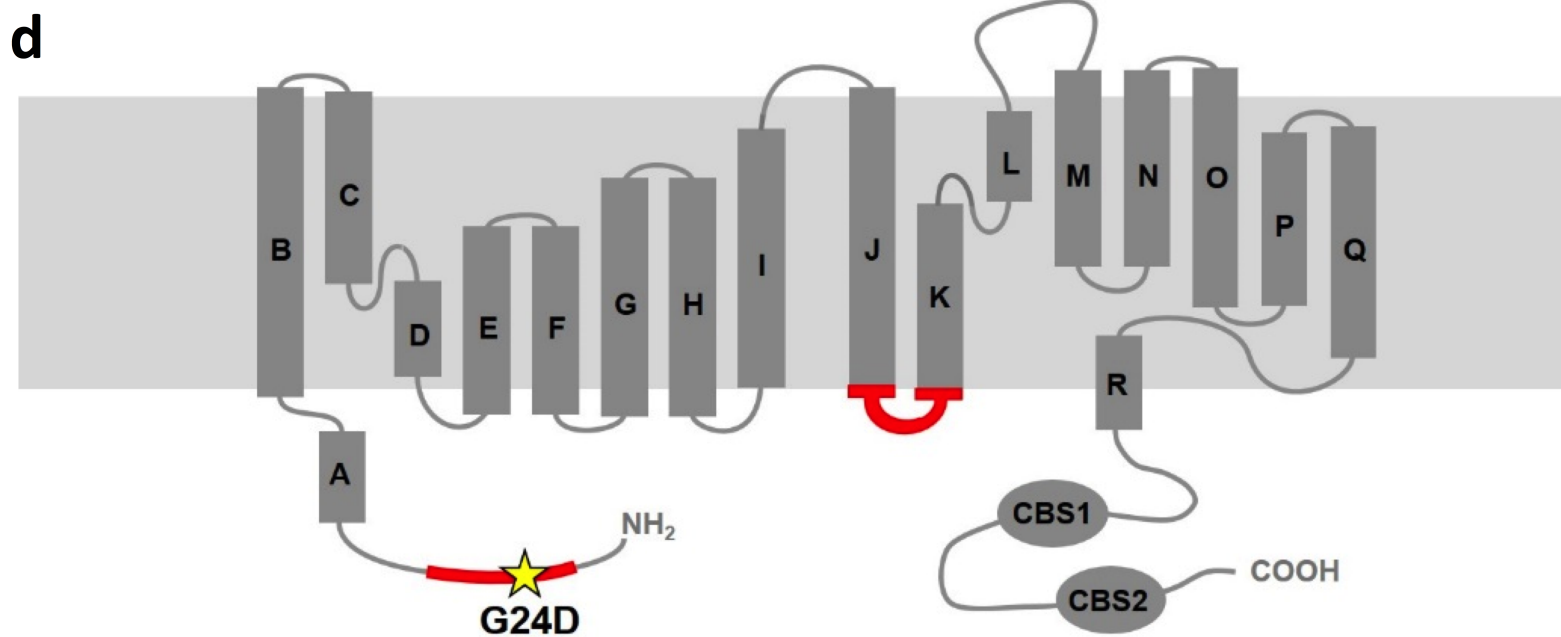
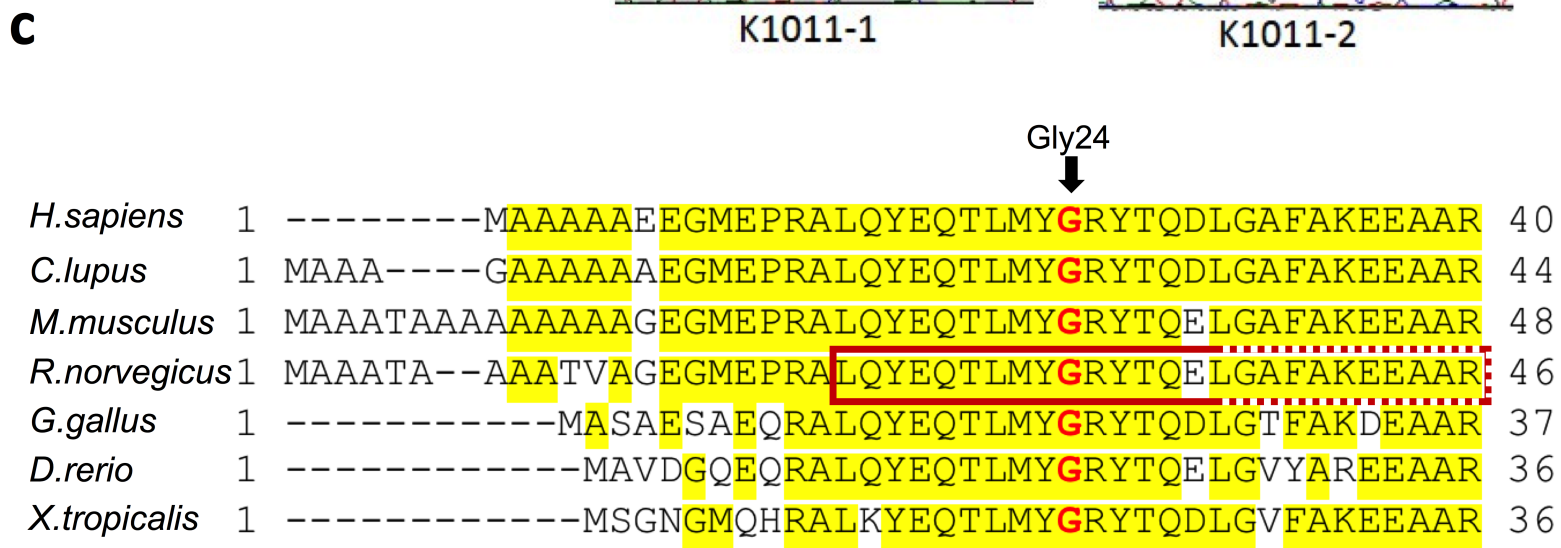
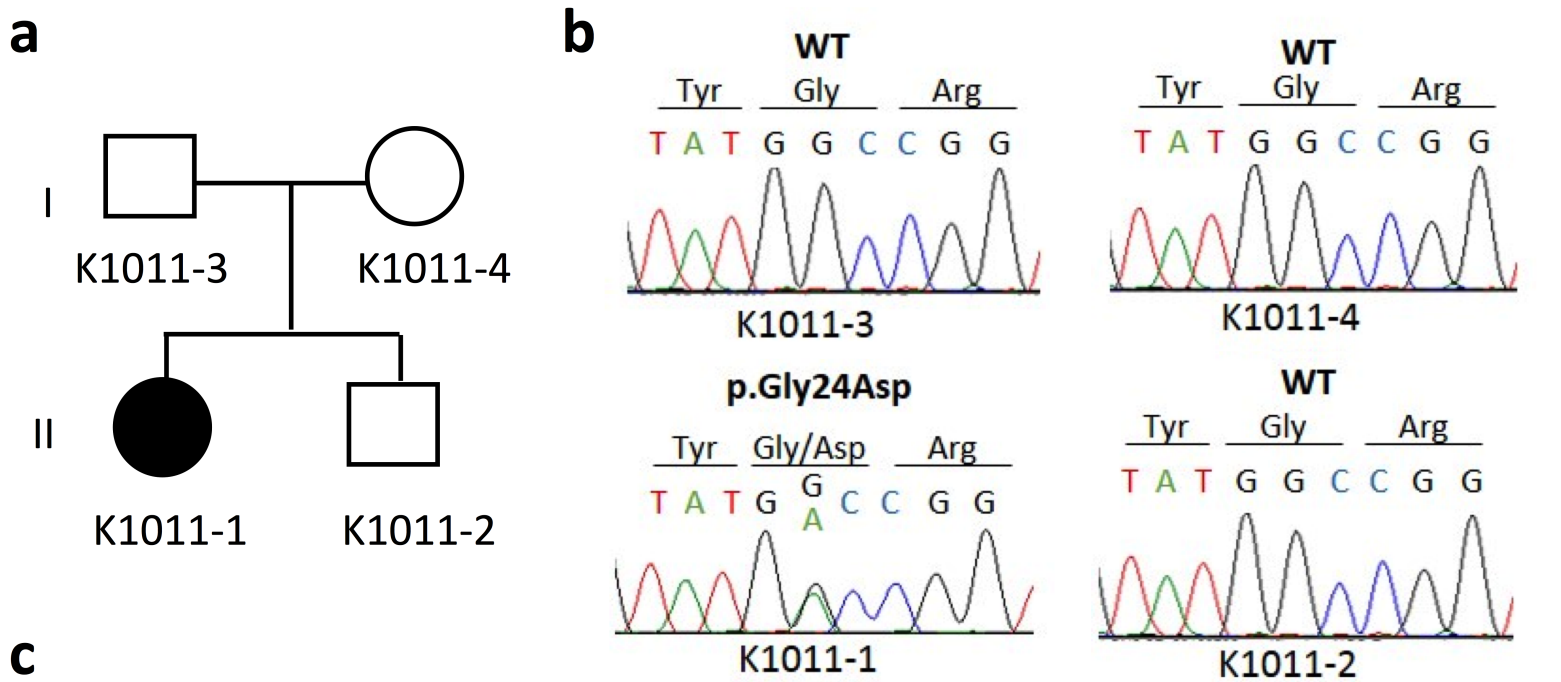


Figure 1

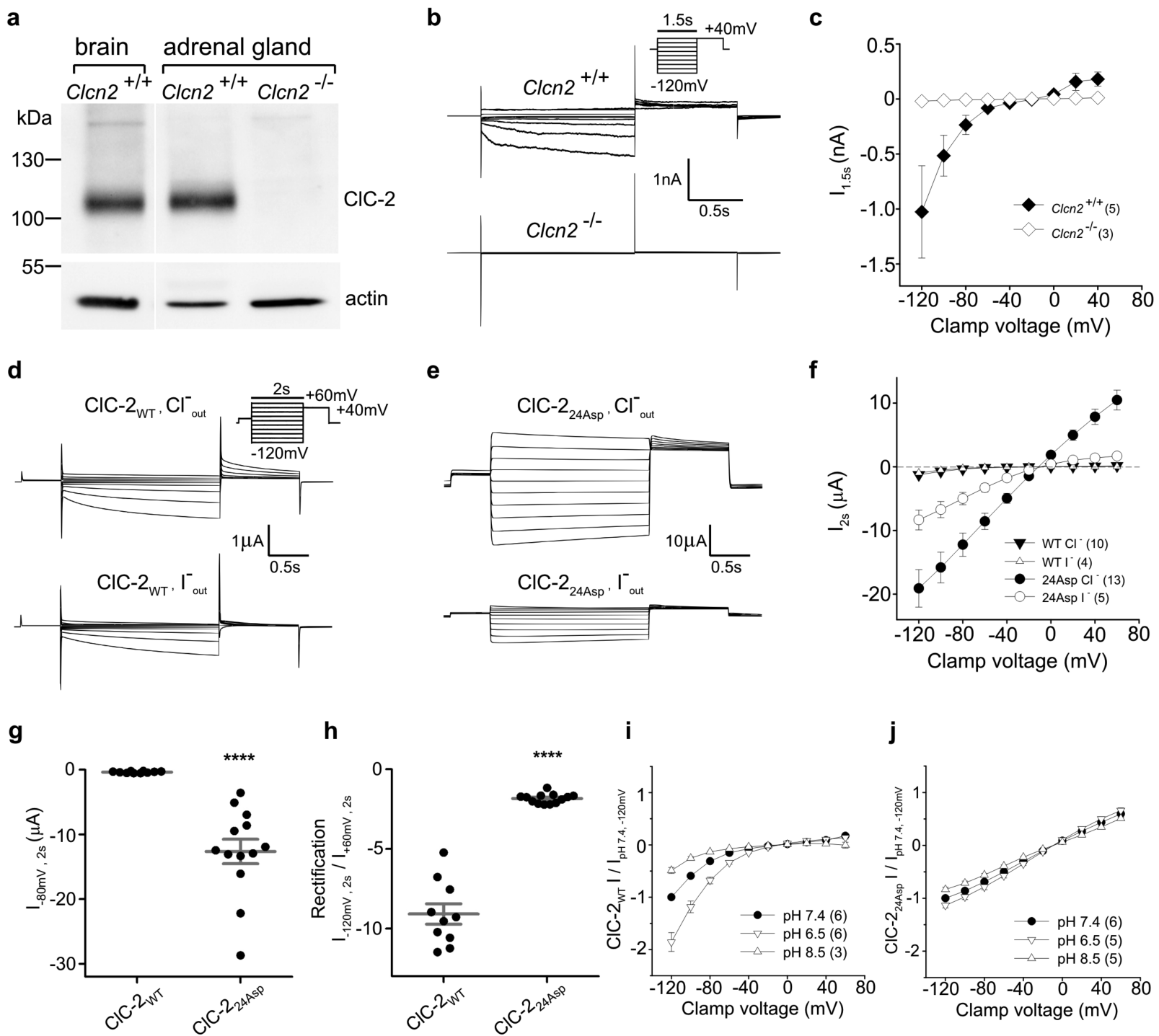


Figure 2

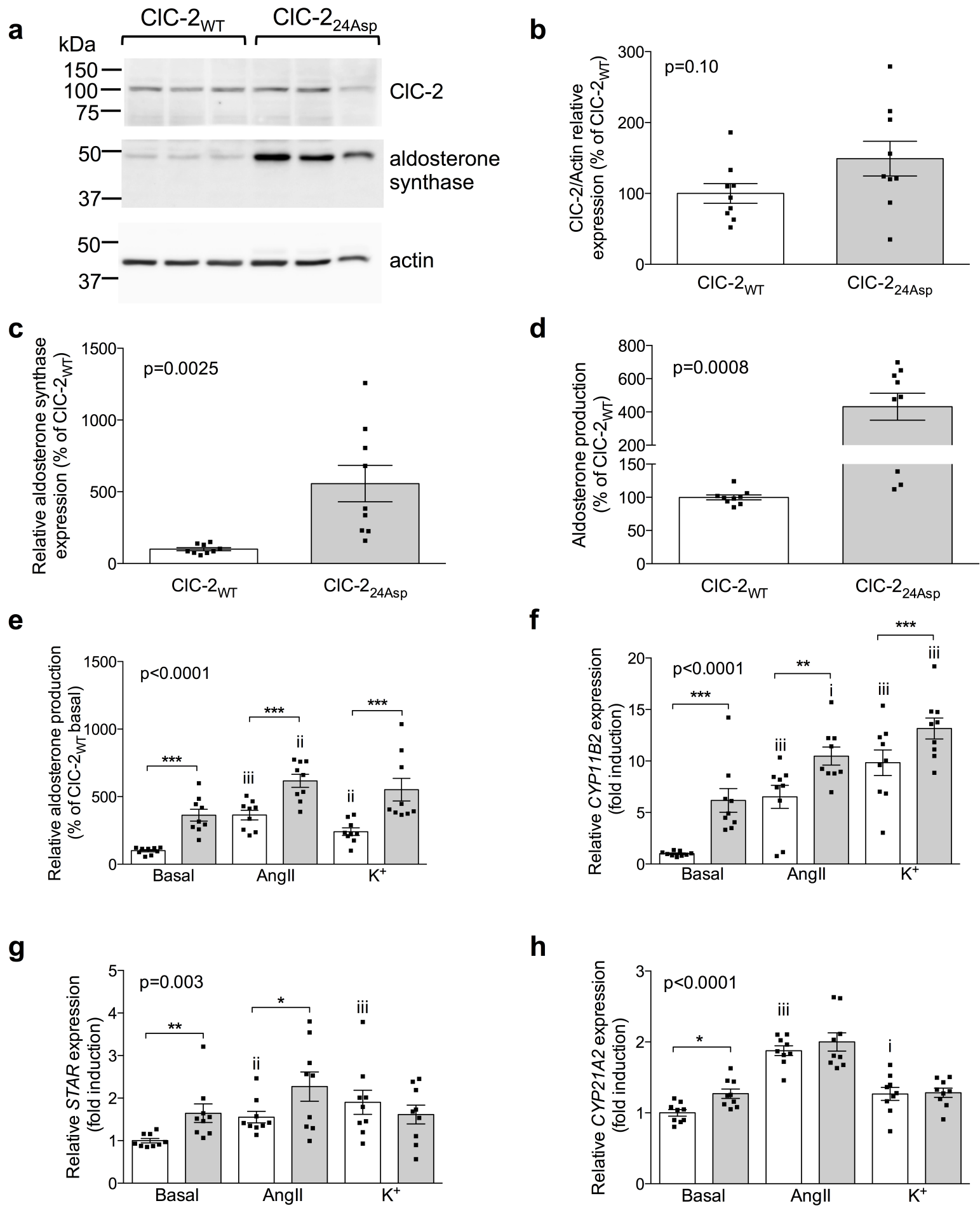


Figure 3

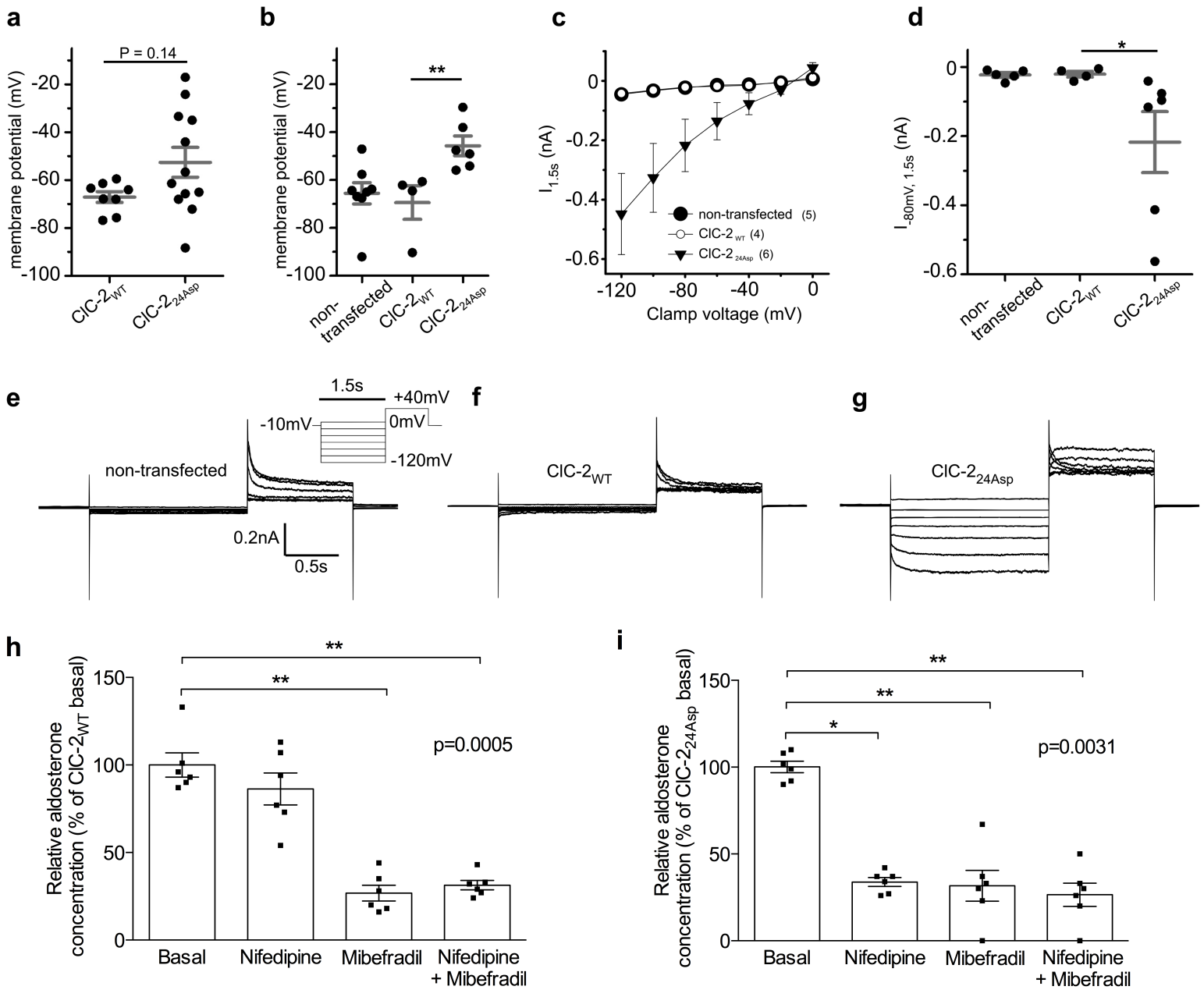


Figure 4

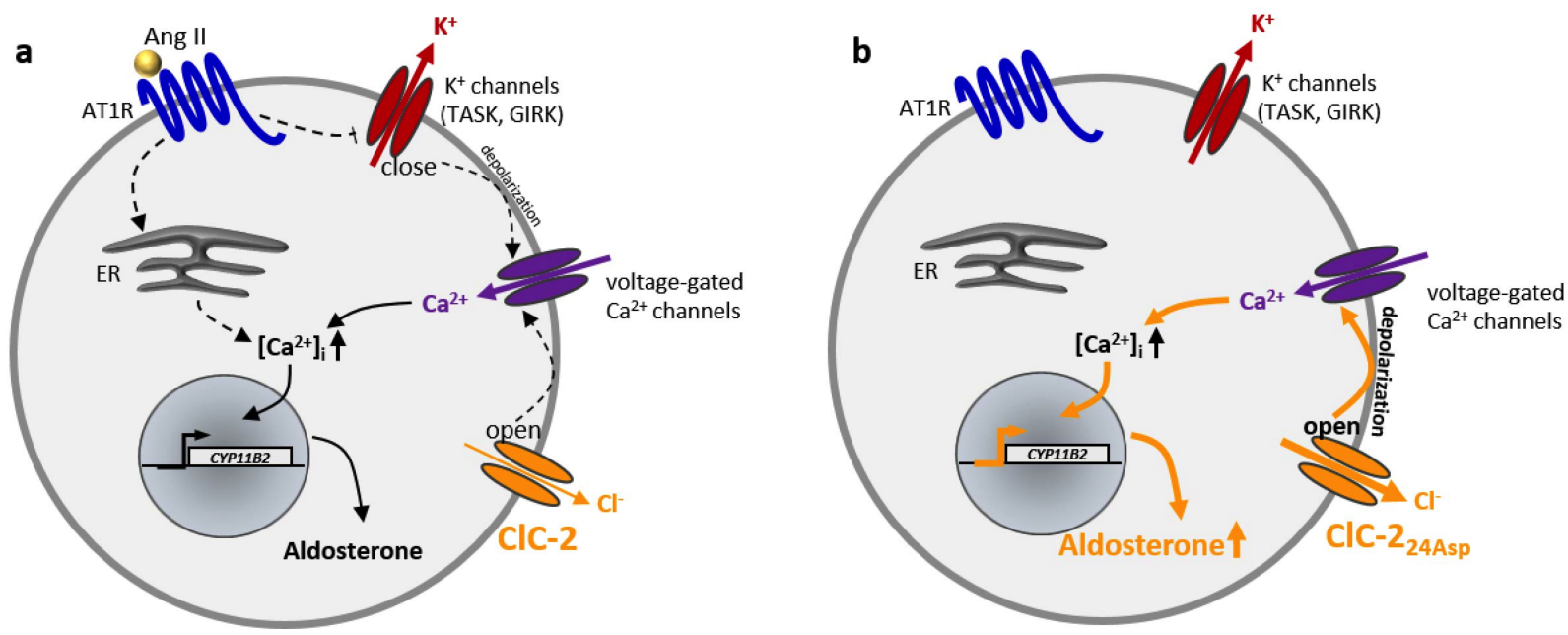


Figure 5